https://doi.org/10.5194/angeo-2023-33
Preprint. Discussion started: 9 November 2023

Annales Geophysicae Discussions
Open Access
EGU

Subauroral Crosstalk in POES/Metop TED proton channels

Jan Maik Wissing[1,2] and Olesya Yakovchuk[2]

[1]Institute for Solar-Terrestrial Physics, DLR Neustrelitz, Neustrelitz, Germany, maik@ionization.de
[2]Institute of Physics, University of Rostock, Rostock, Germany, olesya@ionization.de

Abstract. Particle measurements are used for various purposes. The medium energy channels on the POES/Metop satellites, the MEPED channels, are widely used, for example in atmospheric ionization models, their low energy (eV and keV) counterpart, the TED detector, is not that popular. However the recent rise of the ionization/climate model altitudes will lead to increased interest in these low energy particle measurements.

This paper analyses MEPED and TED particle data from NOAA POES and Metop during 2001–2018 and shows that in particlular the TED proton channels (but also MEPED electron channels and MEPED proton channels P2 and P3) are contaminated by high background levels a $L < 6$. In some channels that may surpass typical auroral levels. We determined a Kp and channel dependent latitude boundary that might be used as (preliminary) cut of the contaminated area.

1 Introduction

More than 50 years the Earth´s radiation belts have been considered to consist of two distinct zones, an inner and outer belt, separated by the so-called slot region (van Allen, 1959, 1983). In 2013 the observations of the Vann Allen Probes have shown a long-lived relativistic electron storage ring in outer belt, third radiation belt, which persisted for four weeks (Baker et al., 2013). The outer belt consists of highly variable and dynamic electron population (0.1–10 MeV), which may extend from L=4 to L=10 (L is the distance in Earth radii at which a magnetic field line crosses the magnetic equatorial plane) and correlate with geomagnetic activity. Its greatest intensity of relativistic electron fluxes is usually between L=3.5 to 5.5 (e.g. Baker et al., 2013). The inner radiation belt is composed mostly of electrons in the range of 100 keV and energetic protons with energies exceeding 100 MeV—trapped by the relatively strong magnetic fields in the region (as compared to the outer belt), located typically at L values between 1.2 and 2.5 and varies slowly over time during quiet time (e.g. Selesnick et al., 2014). However, during strong geomagnetic storms inner belt proton population can change quickly (e.g. Selesnick et al., 2014) or in geographical areas such as the South Atlantic Anomaly, the inner boundary may decline to roughly 200 km above the Earth's surface.

Accurate measurement of energetic particle precipitation is important due to its effects on atmospheric chemistry. Particle precipitation is known to impact atmospheric composition by direct ionisation, production of NOx and HOx and subsequent catalytic destruction of Ozone (Crutzen et al., 1975; Heath et al., 1977; McPeters and Jackman, 1985; Funke et al., 2011). Through the link to Ozone it may also cause changes in the radiation budget and thus atmospheric dynamics.

During the analysis of all available data from POES and Metop for the time period 2001-2018, we found intense contamination from (most likely) high relativistic electrons affecting in particular (low energy) TED proton channels. Inspite of these data

https://doi.org/10.5194/angeo-2023-33
Preprint. Discussion started: 9 November 2023


Annales Geophysicae Discussions

are already corrected for background noise (Green, 2013) from e.g. energetic electrons from the radiation belts at subauroral latitudes, it seems that the background still severely impacts the particle flux.

The purpose of this work is to define a latitudinal cut of the crosstalk dominated area and thus allow a safe application of this data set. Particle flux levels vary with channel and geomagnetic disturbance. Therefore crosstalk and the latitudinal cut may depend on channel and Kp.

The paper is structured as follows: Section 2 describes the used data sets and how they have been processed. In Section 3 we describe the observations of the subauroral flux peak and its Kp dependence while Section 4 discusses crosstalk as a reason for the subauroral flux.

2 Data sets

This section describes the data sets and how the data has been processed.

2.1 Particle data

The particle data origins from the Polar Operational Environmental Satellites (POES) and their successor Meteorological Operational satellite programme (Metop). Both have sun-synchronous orbits at altitudes around 820 km (with $\approx$ 100 minute periods of revolution) and an inclination of $\approx 98.5°$. Even though the satellites have initially been placed in orbits that cross the equator at a fixed local time, either being morning-evening or day-night sector, these orbits were drifting slightly with time, allowing an almost complete local time sector coverage.

The particle detectors on POES and Metop are identical and combined in the Space Environment Monitor SEM-2 (Evans and Greer, 2006). The SEM-2 consists of a low energy instrument, the Total Energy Detector (TED) and the Medium Energy Proton and Electron Detector (MEPED). TED is a cylindrical electrostatic analyser, MEPED is a semiconductor detector with passive shielding.

In total all available data from POES 15, 16, 17, 18, 19 and Metop 01, 02 in the period 2001–2018 has been used, except for POES 16 after 2006 when the TED data is erroneous. The data has been used on a 16 second averaged basis.

This study concentrates on the upward looking (0°) detector as it is seeing precipitating particles in high latitudes. At low latitudes close to the magnetic equator the 0° detector measures mainly trapped particles.

All particle count rates have been converted into differential flux by dividing the energy range and applying satellite/channel specific geometric correction factors (Evans and Greer, 2004). The MEPED electron data has also been converted into differential flux, which needed us to subtract the three nominal integral channels of the MEPED electron data into the resulting two differential channels (30–100 keV and 100–300 keV). The energy ranges of all particle channels are listed in Table 1. Additionally the MEPED electron channels have been set to an error value if high energetic (and potentially cross-talking) protons are detected. This has been performed on 2s basis using the high energetic P7 proton channel from the omni-directional detector as a proxy and setting the error value if it detects more than 2 counts per second. As result MEPED electron measurements during strong proton events are effectively ignored as well as measurements inside the South Atlantic Anomaly.

https://doi.org/10.5194/angeo-2023-33
Preprint. Discussion started: 9 November 2023


Annales Geophysicae Discussions

2.2 Coordinate system

This study uses the family of APEX coordinates (Richmond, 1995). Generally these coordinate systems are based on the International Geomagnetic Reference Field (IGRF). A benefit of the IGRF dependency is that the movement of the poles that manifests in all precipitation features is (mostly) compensated. This allows us to use several years for a spatial long-term approximation of the precipitation flux as well as to apply results for future periods.

As far as it concerns locations on the ground and higher latitudes there is no significant difference to the more popular Altitude Adjustment Corrected GeoMagnetic (AACGM) coordinates (practically identical pole-ward of 50°, see Fig. 7 in Laundal and Richmond, 2017).

For positions above the ground however the APEX coordinates are more suitable for the description of charged particles. The APEX coordinates follow the magnetic field-lines from their foot-points further up, therefore a charged particle should always stay on the same APEX position during it's bounce motion. Consequently in APEX coordinates the altitude of the (satellite) measurement does not vary the location of a particle.

Without further modification the reference altitude for the footpoints of the magnetic field-lines is the ground level, but the APEX coordinates also allow for a manual choice of the reference altitude. In fact, we used 110 km as reference altitude because this is approximately the altitude where atmospheric interactions become dominant against the magnetic field. Hence the coordinate system is called *APEX 110 km* in the rest of the study.

2.3 Kp-binning of particle data

The planetary K-index (Kp, Bartels et al., 1939) represents the geomagnetic activity in a 3-hourly quasi-logarithmic index (ranging from 0 to 9). It is based on 13 geomagnetic observatories between 44° and 60° northern and southern geomagnetic latitude and is sensitive to different current systems (e.g. the ring current). Therefore is describes the magnetospheric activity from a global point of view. In our work the particle data has been split up into 7 Kp-level groups: 0–0.7, 1–1.7, 2–2.7, 3–3.7, 4–4.7, 5–5.7 and 6–9.

3 Observation of suspicious particle fluxes outside typical precipitation areas

A local flux maximum separated from the auroral precipitation and the SAA has already been shown in Yakovchuk and Wissing (2019, Fig. 1). The aim of this section is to determine which channels and which regions are affected by enhanced (but probably unrealistic) subauroral particle flux.

Fig. 1 shows the binned average particle flux in a TED proton channel for the years 2001 to 2018 selected by geomagnetic disturbance (left: Kp=0–0.7, right: Kp=4–4.7). The suspicious flux appears at about 60° North and South and is most prominantly seen at longitudes that also cross the SAA (Southern part centered at about 60° E).

https://doi.org/10.5194/angeo-2023-33
Preprint. Discussion started: 9 November 2023

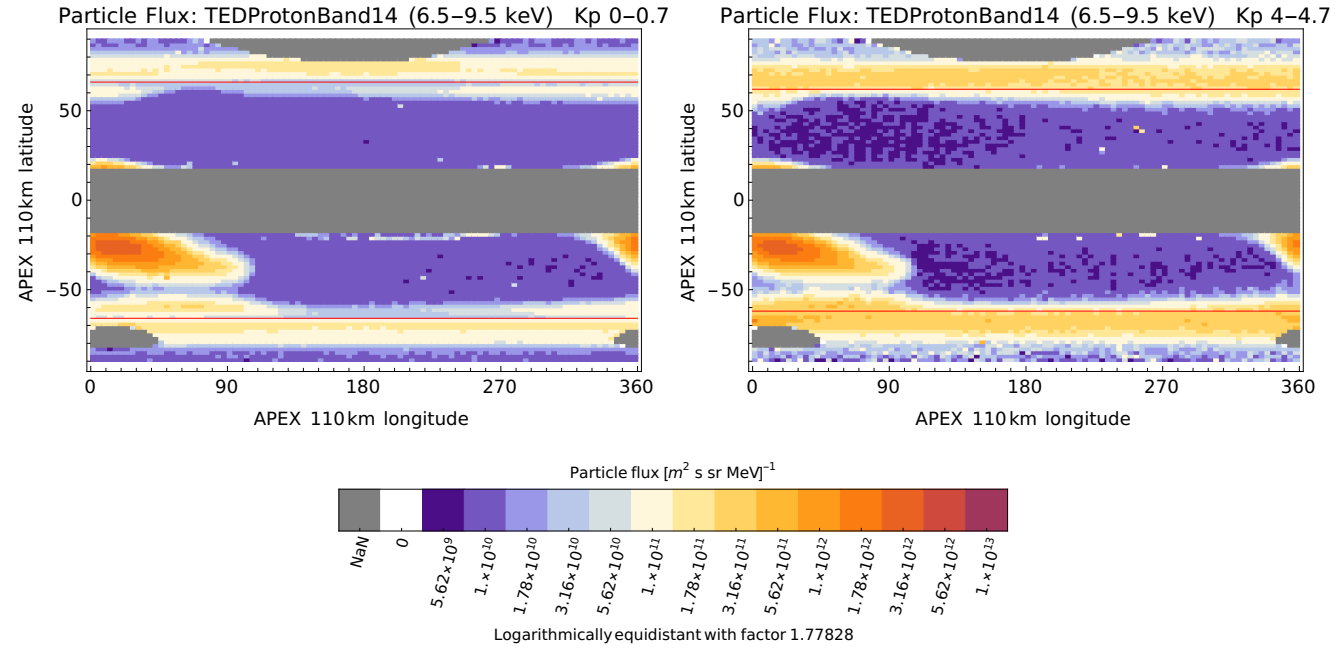

Figure 1. Spatial flux distribution of a TED proton channel for selected Kp levels (low Kp: left, medium Kp: right) averaged over the years 2001-2018.

At low Kp levels (see Fig. 1, left) the spatial flux pattern (for all TED proton channels) shows a clear minimum/separation (indicated by the red line) between auroral oval and the subauroral peak. With increasing Kp (see Fig. 1, right) the separation becomes less visible as the flux minimum disappears. For higher Kp levels (Kp$\geq$ 5) there is no obvious subauroral peak.

Fig. 2 shows a cross-section of TED proton band 11 through 60°E based on the same multi-year binning. The latitude axis is stitched together: in mod. APEX 110 km coordinates latitudes are restricted being $> 18°$. Different Kp levels have been selected to illustrate the evolution with geomagnetic disturbance. While the maximum intensity of the subauroral peak is fixed at about 56-60° North and South, the broadening of the auroral precipitation and its intensification shifts the location of the minimum between auroral flux and subauroral peak equator-ward for higher Kp levels. In extreme cases e.g. at TED proton band 14 and Kp 4–4.7 the auroral precipitation even moves into the crosstalk area (see Fig. 1, right). However, due to its latitudinal extend (and flux differences as in case of TED proton band 14) parts of it are still visible. Note that 60° E does not pass the northern subauroral peak which anyway is less intense than the southern one.

Table 1 lists all channel and Kp combinations where enhanced subauroral fluxes have been detected in addition to the latitude of the minimum poleward of the subauroral peak. Obviously the appearance of a subauroral peak is limited to low geomagnetic disturbance. It is seen in all TED proton channels, while no impact on the electron counterpart has been identified here. Some MEPED channels show subauroral peaks as well but much weaker and restricted to Kp 0–1.7 or even 0–0.7.

https://doi.org/10.5194/angeo-2023-33
Preprint. Discussion started: 9 November 2023

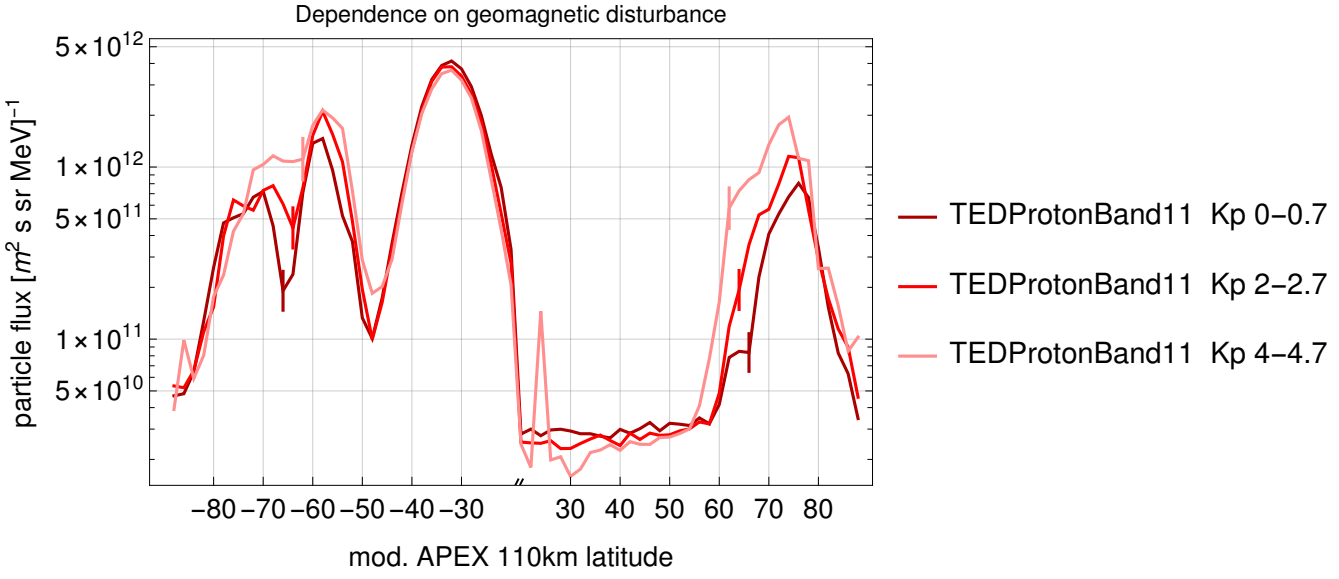

Figure 2. Cross-section at 60° E for TED proton band 11 during different levels of geomagnetic disturbance. The vertical lines (in the same color as the according graph) indicate the minimum between auroral and subauroral peak.

4 Discussion

Fig. 3 shows the mean particle fluxes for 2013 and Kp≤ 0.7 along 60° magnetic longitude against L shell. Year 2013 has been chosen as NOAA changed its data format and the TED background counts (drawn in black and gray) which are used for correction (Green, 2013) can be exported easily. The background counts are significantly increased at two locations, first L≤ 2 which corresponds to the SAA. The SAA is known for intense particle crosstalk affecting in particular the MEPED electron channels (Peck et al., 2015). A second background count peak is located in the range L$= 3-6$ with a maximum at L$= 4$ ($\approx 60°$ N/S). According to Li et al. (2001); Baker et al. (2013); Baker et al. (2019) this agrees to the occurence of highly relativistic electrons in the radiation belts. Energetic electron crosstalk also explains the Kp dependence as Turner et al. (2012) point out that the radiation belt electron flux dropc by orders of magnitude during geomagnetic storms.

The electron background counts are increased as well, however not as strong as the proton background counts. Given that the natural TED electron fluxes are typically higher than the proton fluxes (see at L> 7) the impact of crosstalk on TED electron channels is smaller. In case of TED electron band 4 it is not noticeable. TED electron band 11 and 14 should be affected to some extend, but there is no clear spatial separation to the auroral flux. In contrast to that, all TED proton channels show a clear maximum in place with the increased background counts at L=4. Note that we used the processed “ted_ele_tel0_flux_4” (and similar labelling for protons and other bands) which should have already been corrected for background counts according to Green (2013). The MEPED instrument shows the crosstalk characteristics for the lowest channels as well. While the channels

https://doi.org/10.5194/angeo-2023-33
Preprint. Discussion started: 9 November 2023

Annales Geophysicae Discussions
Open Access
EGU

	instrument	channel	energy range	Separation of the contamination area at Kp						
				0–0.7	1–1.7	2–2.7	3–3.7	4–4.7	5–5.7	6–9
electrons	TED	band 4	154–224 eV	-	-	-	-	-	-	-
		band 8	688–1000 eV	-	-	-	-	-	-	-
		band 11	2.115–3.075 keV	-	-	-	-	-	-	-
		band 14	6.503–9.457 keV	-	-	-	-	-	-	-
	MEPED	mep0e1-e2	30–100 keV	62°†	-	-	-	-	-	-
		mep0e2-e3	100–300 keV	64°	62°	-	-	-	-	-
protons	TED	band 4	154–224 eV	66°	64°	62°	60°	58°	-	-
		band 8	688–1000 eV	66°	64°	64°	62°	62°	-	-
		band 11	2.115–3.075 keV	66°	66°	64°	64°	62°	-	-
		band 14	6.503–9.457 keV	66°	64°	64°	62°	62°	-	-
	MEPED	mep0P1	30–80 keV	-	-	-	-	-	-	-
		mep0P2	80–240 keV	62°	-	-	-	-	-	-
		mep0P3	240–800 keV	62°	62°†	-	-	-	-	-
		mep0P4	0.8–2.5 MeV	-	-	-	-	-	-	-
		mep0P5	2.5–6.9 MeV	-	-	-	-	-	-	-

Table 1. Channel and Kp combinations that show enhanced subauroral flux and the location of the minimum between auroral and subauroral peaks. As identified visually on spatial maps like Fig. 1. The latitude applies for North and South. † *almost invisible*

mep0P2, mep0P3, mep0e1-e2corr and mep0e2-e3corr have been identified already in Tab. 1, Fig. 3 supports crosstalk in mep0P1 as well.

Are all these channels sensitive to highly relativistic electron crosstalk? For TED channels, the TED background counts and the typical location of the electron radiation belt at L=4 give a strong indication. For the MEPED detector (Yando et al., 2011) performed Geant4 simulations that revealed a high sensitivity for energetic (radiation belt) electrons in the proton channels mep0P1, mep0P2 and mep0P3. The MEPED electron channels mep0e1 to mep0e3 are sensitive to high energetic electron by design (compare Yando et al., 2011, for modeled sensitivity). As they are subtracted in this study the crosstalk is minimized but probably not completely removed.

On the other side Selesnick et al. (2020) showed that especially during periods of low pitch angle diffusion (equivalent to low Kp) most of the detector counts at L=4 in the 0 degree detector result from trapped or quasi-trapped (out of nominal field-of-view) electrons. In so far a determination of the precipitating flux based on the 0 degree detector would lead to a significant overestimation. Therefore the crosstalk might not be restricted to relativistic electrons, but also includes out-of-view contamination.

https://doi.org/10.5194/angeo-2023-33
Preprint. Discussion started: 9 November 2023

Annales Geophysicae Discussions

5 Conclusions

1. We investigated a subauroral particle flux maximum (located at $\approx 60^\circ$ N/S equivalent to L=4 and a longitudinal focus at 0–100° East, southward of the SAA), which we attributed to crosstalk contamination of relativistic radiation belt electrons.

2. Channels that show subauroral crosstalk contamination are in particular all TED protons, but also the lower MEPED proton channels: mep0P1 (according to Fig. 3), mep0P2 and mep0P3 and the MEPED electron channels: mep0e1-e2 and mep0e2-e3. For the TED electron channels Fig. 3 indicates that crosstalk might be an issue. But due to higher natural fluxes and smaller background count rates the impact is much smaller than on the proton detector. At least TED electron band 4 seems to be free from crosstalk at subauroral latitudes.

3. The TED crosstalk correction from NOAA (Green, 2013) based on background counts seems to be insufficient for a complete removal of the radiation belt electron crosstalk.

4. The observed particle flux in the contaminated subauroral maximum can be more than factor 2 higher than typical auroral flux (TED proton band 11), which shows the need of an improved correction algorithm.

5. As a preliminary measure, the region of intense particle crosstalk may be removed by a latitudinal cut as provided in Table 1 even though this is limited to channels with a clear crosstalk peak.

Author contributions. Both authors contributed equally to analysis and paper writing.

Competing interests. The authors declare that they have no conflict of interest.

Acknowledgements. This work is funded by the German Science Foundation (DFG project WI4417/2-1). The authors acknowledge the NOAA National Centers for Environmental Information (https://ngdc.noaa.gov/stp/satellite/poes/dataaccess.html) for the POES and Metop particle data used in this study. The Kp-index is provided from GFZ Potzdam (https://kp.gfz-potsdam.de).

https://doi.org/10.5194/angeo-2023-33
Preprint. Discussion started: 9 November 2023

Annales Geophysicae Discussions

References

Baker, D. N., Kanekal, S. G., Hoxie, V. C., Henderson, M. G., Li, X., Spence, H. E., Elkington, S. R., Friedel, R. H. W., Goldstein, J., Hudson, M. K., Reeves, G. D., Thorne, R. M., Kletzing, C. A., and Claudepierre, S. G.: A Long-Lived Relativistic Electron Storage Ring Embedded in Earth's Outer Van Allen Belt, Science, 340, 186–190, https://doi.org/10.1126/science.1233518, 2013.

Baker, D. N., Hoxie, V., Zhao, H., Jaynes, A. N., Kanekal, S., Li, X., and Elkington, S.: Multiyear Measurements of Radiation Belt Electrons: Acceleration, Transport, and Loss, Journal of Geophysical Research (Space Physics), 124, 2588–2602, https://doi.org/10.1029/2018JA026259, 2019.

Bartels, J., Heck, N. H., and Johnston, H. F.: The three-hour-range index measuring geomagnetic activity, Terrestrial Magnetism and Atmospheric Electricity, 44, 411–454, https://doi.org/10.1029/TE044i004p00411, 1939.

Crutzen, P. J., Isaksen, I. S. A., and Reid, G. C.: Solar Proton Events: Stratospheric Sources of Nitric Oxide, Science, 189, 457–459, https://doi.org/10.1126/science.189.4201.457, 1975.

Evans, D. S. and Greer, M. S.: Polar Orbiting Environmental Satellite Space Environment Monitor - 2, Instrument Descriptions and Archive Data Documentation, National Oceanic and Atmospheric Administration, NOAA Space Environ. Lab, Boulder, Colorado, USA, version 1.4b, including TED calibrations, 2004.

Evans, D. S. and Greer, M. S.: Polar Orbiting Environmental Satellite Space Environment Monitor - 2, Instrument Descriptions and Archive Data Documentation, National Oceanic and Atmospheric Administration, NOAA Space Environ. Lab, Boulder, Colorado, USA, version 2.0, 2006.

Funke, B., Baumgaertner, A., Calisto, M., Egorova, T., Jackman, C. H., Kieser, J., Krivolutsky, A., López-Puertas, M., Marsh, D. R., Reddmann, T., Rozanov, E., Salmi, S.-M., Sinnhuber, M., Stiller, G. P., Verronen, P. T., Versick, S., von Clarmann, T., Vyushkova, T. Y., Wieters, N., and Wissing, J. M.: Composition changes after the "Halloween" solar proton event: the High Energy Particle Precipitation in the Atmosphere (HEPPA) model versus MIPAS data intercomparison study, Atmospheric Chemistry and Physics, 11, 9089–9139, https://doi.org/10.5194/acp-11-9089-2011, 2011.

Green, J.: TED Data Processing - ALGORITHM THEORETICAL BASIS DOCUMENT - Version 1.0, Tech. rep., NOAA NESDIS-NGDC, https://ngdc.noaa.gov/stp/satellite/poes/docs/NGDC/TEDprocessingATBD_V1.doc, 2013.

Heath, D. F., Krueger, A. J., and Crutzen, P. J.: Solar proton event - Influence on stratospheric ozone, Science, 197, 886–889, https://doi.org/10.1126/science.197.4306.886, 1977.

Laundal, K. M. and Richmond, A. D.: Magnetic Coordinate Systems, Space Sci. Rev., 206, 27–59, https://doi.org/10.1007/s11214-016-0275-y, 2017.

Li, X., Baker, D. N., Kanekal, S. G., Looper, M., and Temerin, M.: Long term measurements of radiation belts by SAMPEX and their variations, Geophysical Research Letters, 28, 3827–3830, https://doi.org/https://doi.org/10.1029/2001GL013586, 2001.

McPeters, R. D. and Jackman, C. H.: The response of ozone to solar proton events during solar cycle 21: The observations, Journal of Geophysical Research: Atmospheres, 90, 7945–7954, https://doi.org/10.1029/JD090iD05p07945, 1985.

Peck, E. D., Randall, C. E., Green, J. C., Rodriguez, J. V., and Rodger, C. J.: POES MEPED differential flux retrievals and electron channel contamination correction, Journal of Geophysical Research: Space Physics, 120, 4596–4612, https://doi.org/10.1002/2014JA020817, 2015.

Richmond, A. D.: Ionospheric Electrodynamics Using Magnetic Apex Coordinates., Journal of Geomagnetism and Geoelectricity, 47, 191–212, https://doi.org/10.5636/jgg.47.191, 1995.

https://doi.org/10.5194/angeo-2023-33
Preprint. Discussion started: 9 November 2023

Selesnick, R. S., Baker, D. N., Jaynes, A. N., Li, X., Kanekal, S. G., Hudson, M. K., and Kress, B. T.: Observations of the inner radiation belt: CRAND and trapped solar protons, Journal of Geophysical Research (Space Physics), 119, 6541–6552, https://doi.org/10.1002/2014JA020188, 2014.

Selesnick, R. S., Tu, W., Yando, K., Millan, R. M., and Redmon, R. J.: POES/MEPED Angular Response Functions and the Precipitating Radiation Belt Electron Flux, Journal of Geophysical Research: Space Physics, 125, e2020JA028 240, https://doi.org/https://doi.org/10.1029/2020JA028240, e2020JA028240 10.1029/2020JA028240, 2020.

Turner, D. L., Shprits, Y., Hartinger, M., and Angelopoulos, V.: Explaining sudden losses of outer radiation belt electrons during geomagnetic storms, Nature Physics, 8, 208–212, https://doi.org/10.1038/nphys2185, 2012.

van Allen, J. A.: The Geomagnetically Trapped Corpuscular Radiation, Journal of Geophysical Research, 64, 1683–1689, https://doi.org/10.1029/JZ064i011p01683, 1959.

van Allen, J. A.: Origins of magnetospheric physics., University of Iowa Press, 1983.

Yakovchuk, O. and Wissing, J.: Magnetic local time asymmetries in precipitating electron and proton populations with and without substorm activity, Annales Geophysicae, 37, 1063–1077, https://doi.org/10.5194/angeo-37-1063-2019, 2019.

Yando, K., Millan, R. M., Green, J. C., and Evans, D. S.: A Monte Carlo simulation of the NOAA POES Medium Energy Proton and Electron Detector instrument, Journal of Geophysical Research: Space Physics, 116, https://doi.org/10.1029/2011JA016671, 2011.

https://doi.org/10.5194/angeo-2023-33
Preprint. Discussion started: 9 November 2023

Annales Geophysicae Discussions
Open Access
EGU

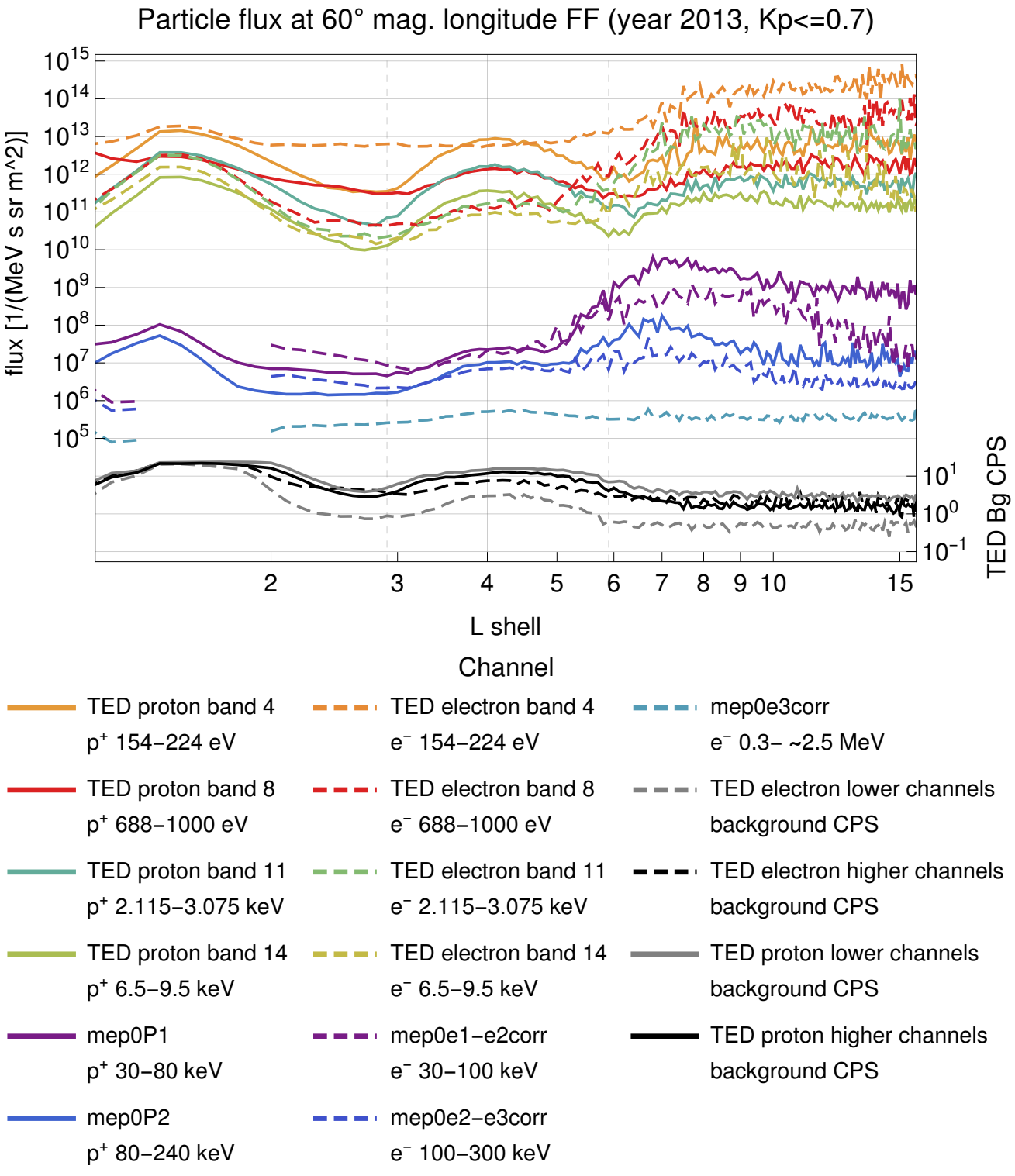

Figure 3. High background counts in L$\leq$ 2 (SAA) and in L= 3 – 6 (subauroral peak) co-incide with intense particle counts in TED proton channels and some MEPED channels.